

State-selective differential cross sections for single and double electron capture in $\text{He}^{+,2+}$ -He and p -He collisions

M. S. Schöffler,^{1,2,*} J. Titze,¹ L. Ph. H. Schmidt,¹ T. Jahnke,¹ N. Neumann,¹ O. Jagutzki,¹ H. Schmidt-Böcking,¹ R. Dörner,¹ and I. Mančev³

¹*Institut für Kernphysik, Universität Frankfurt, 60438 Frankfurt, Germany*

²*Lawrence Berkeley National Laboratory, Berkeley, California 94720, USA*

³*Department of Physics, Faculty of Sciences and Mathematics, University of Niš, P.O. Box 224, 18000 Niš, Serbia*

(Received 22 April 2009; published 10 June 2009)

Using the cold target recoil ion momentum spectroscopy technique, we have measured state-selective projectile scattering angles for single and double electron captures in collisions of protons and $\text{He}^{1,2+}$ projectiles with a helium target for incident energies of 60–630 keV/u. We also report theoretical results obtained by means of four-body one-channel distorted-wave models (continuum distorted-wave Born final state, continuum distorted-wave Born initial state, and Born distorted wave) and find mixed agreement with the measured data.

DOI: [10.1103/PhysRevA.79.064701](https://doi.org/10.1103/PhysRevA.79.064701)

PACS number(s): 34.70.+e

I. INTRODUCTION

For many decades electron transfer processes in ion-atom collisions have been investigated theoretically and experimentally because of their fundamental nature [1]. Most of the early works focused on the absolute cross sections. State of the art experiments today give access to fully differential cross sections. For capture reactions a kinematically complete experiment involves simultaneous detection of the electronic state of projectile and target as well as the scattering angle, which is related to the impact parameter.

The key variable controlling the mechanism responsible for the electron transfer is the ratio of orbital electron and projectile velocity v_p . At small velocities electron transfer proceeds via the formation of intermediate molecular states. At intermediate velocities capture is governed by the overlap of the wave functions of initial target and final projectile state in momentum space, displaced by the projectile velocity (Oppenheimer-Brinkman-Kramers, OBK, capture [2,3]). At even higher velocities electron capture is more likely dominated by the Thomas process, an interatomic double scattering, which accelerates the target electron to projectile velocity and leads to a distinct structure [4–7] in the scattering angle. For our experiments we focused on a projectile velocity regime (1.5–5 a.u.) where the OBK capture dominates and the Thomas process should be a very small contribution.

Previous theoretical calculation mainly focused on the ground-state transfer ($1s$ - $1s$), while most experiments averaged over all excited states of target and projectile. Summation of the scattering-angle dependence over excited states of projectile and/or target can wash out much of the structure in the individual channels [8] and obscure the comparison to theory. In our experiment we used the cold target recoil ion momentum spectroscopy (COLTRIMS) technique [9–11] that measures simultaneously the Q value (the change of the binding energies) of the electron transfer and the projectile scattering angle with very high precision. As the ground-state transfer is the most dominant channel, we focus on this.

II. EXPERIMENT

The experiments were conducted at the 2.5 MV van de Graaff accelerator at the Institut für Kernphysik, University of Frankfurt. The final state after single (double) electron capture is given by a He^+ (He^{2+}) recoiling-target ion and the coincident-reduced charged projectile. The target is a two-stage supersonic gas jet. Using a 30 μm jet nozzle and a driving pressure of 30 bar we achieved a gas jet diameter of 1.5 mm and a jet density of 5×10^{11} helium atoms/cm² at the intersection with the ion beam. This corresponds to a target momentum spread of 0.1 a.u. in all three dimensions. The projectile beam (H^+ , He^+ , or He^{2+}) was collimated by two sets of adjustable slits to a beam cross section of 0.5×0.5 mm² at the target. Electrostatic deflectors upstream and downstream of the target jet were used to eliminate charge state impurities and to separate the primary beam from projectile products. The latter were detected by a 40 mm position- and time-sensitive multichannel plate (MCP) detector with delay-line readout [12].

Perpendicular to the incident projectile beam direction we applied a weak homogeneous electrostatic field of 4.8 V/cm to project the $\text{He}^{1,2+}$ recoil ions onto another position- and time-sensitive MCP detector (80 mm diameter) with delay-line anode. To maximize the resolution by minimizing the perturbing influence of the extended reaction volume a three-dimensional time- and space-focusing field geometry was used (see Fig. 2 in [13]). The overall distance from target to recoil ion detector was 1.4 m, which yielded flight times of 19 μs for He^+ ions and 4π solid angle collecting for transverse momenta up to 9 a.u. From the recoil ion time of flight and the position of impact we can derive the initial three-dimensional momentum vector.

Along the projectile beam axis the momentum of the recoil ion p_{\parallel} is directly related to the number of transferred electrons (n_e) and the total Q value of the reaction [8]

$$p_{\parallel} = -\frac{Q}{v_p} - \frac{n_e v_p}{2}. \quad (1)$$

Each final electronic state (i.e., different Q value) corresponds to a well-defined discrete longitudinal ion momentum p_{\parallel} (see Fig. 1). The width of these peaks (0.1 a.u.) is the

*schoeffler@atom.uni-frankfurt.de

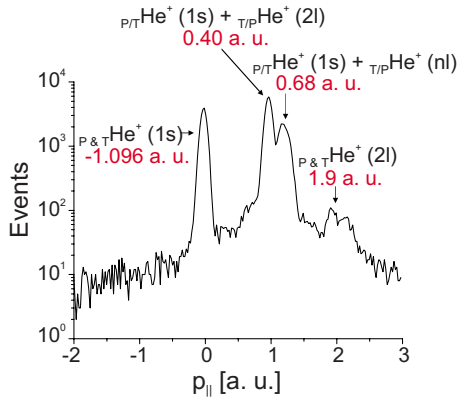


FIG. 1. (Color online) Longitudinal recoil ion momenta (p_{\parallel}) for the single capture in the collision system $\text{He}^{2+}(\text{He})$ at 60 keV/u. The subscript letters P (T) indicate the particle corresponding to the final electronic state in the bracket. The final states “nl” include all states for $n \geq 3$. The numbers shown present the Q value of the reaction. For the two peaks around $p_{\parallel} \approx 1$ a.u. one cannot distinguish whether the projectile (p) or the target (t) is excited, only that one of both is.

overall resolution—a result of the target temperature and the spectrometer and detector properties. The measured values for all final states have been normalized to total cross sections, taken from [14]. The projectile scattering angles (i.e., transverse momenta) are measured with a lower resolution than achieved for the coincident recoiling target ions. Therefore we used them only for background suppression by checking for momentum conservation in the plane perpendicular to the initial beam axis. We deduced the reported projectile scattering angles θ from the coincident momentum transferred to the recoiling target ion ($\text{He}^{1,2+}$).

III. THEORY

In this paper, we shall use three four-body methods for describing single and double electron captures. First, the four-body Born distorted-wave (BDW) model [15,16] is employed for investigating double charge exchange. The BDW is hybrid-type model, which in the entrance and exit channels, coincides with the continuum distorted-wave four-body model (CDW 4B) [17] and four-body boundary-corrected first Born approximation (CB1 4B) [18] method, respectively, so that BDW model includes continuum intermediate states of the captured electrons only in one channel. So far, the BDW model was applied for calculating the differential cross section for double electron capture in collisions between the He^{2+} ions and He atoms at $E=1.5$ MeV [16]. In the present paper we have tested four-body BDW theory at intermediate impact energies. Next, the continuum distorted-wave Born initial state (CDW BIS) approximation [19] and the continuum distorted-wave Born final state (CDW BFS) [20] are utilized for calculating differential cross sections for single electron capture. Both methods employed the scattering wave function from the four-body continuum distorted wave (CDW) [21] method in one of the two channels (CDW BIS in the exit channel, whereas CDW BFS in the entrance channel). For the other channel, the CDW BIS and CDW

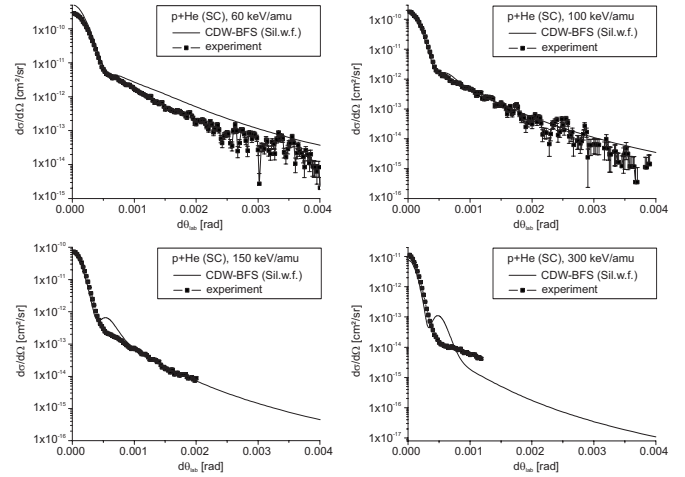


FIG. 2. The differential cross sections $d\sigma_{if}/d\Omega(\text{cm}^2/\text{sr})$ as a function of scattering angle $\theta(\text{rad})$ for single-electron capture to the ground state in H^+-He collisions at 60, 100, 150, and 300 keV/u in the laboratory system. ■: experiment; solid line CDW BFS model (present computation).

BFS methods use the corresponding wave functions of the four-body first Born approximation (CB1).

The main idea of these hybrid-type models is to approximate the exact wave function in one of the channels, by using a simple analytical function, which can well describe the principal interaction region and to preserve correct boundary conditions in both channels. Hence, according to these models the captured electrons are treated in an asymmetrical manner in the entrance and exit channels. Different four-body methods for various inelastic high-energy ion-atom collisions have recently been analyzed in the review paper of Belkić *et al.* [1].

IV. RESULTS AND DISCUSSION

Theoretical results for differential cross sections for single electron capture in H^+-He collisions at impact energies 60, 100, 150, and 300 keV obtained by means of four-body CDW BFS model are compared to the measured data in Fig. 2. The theoretical results in Fig. 2 are obtained by means of two-parameter (Silverman *et al.* [22]) orbitals for the initial helium bound state. The computations are performed also with the help of the simplest one-parameter orbitals of Hylleraas [23] as well as four-parameter wave functions of Löwdin [24]. We find that the differential cross section is rather insensitive to the choice of the bound-state wave functions, since the differences between the results are less than 20%. Scattering angles below 0.55 mrad are known to be dominated by momentum transfer mediated by the electron (see [7,25,26] for capture reactions) while in all larger deflection angles the scattering is dominated by momentum exchange between the nuclei. The theory yields good agreement in shape and in absolute height with the experimental data at small scattering angles for all energies, in agreement with the findings in [27–29]. However, for larger scattering angles theory predicts slightly different angular and v_p dependencies. Particularly the CDW BFS approximation predicts a

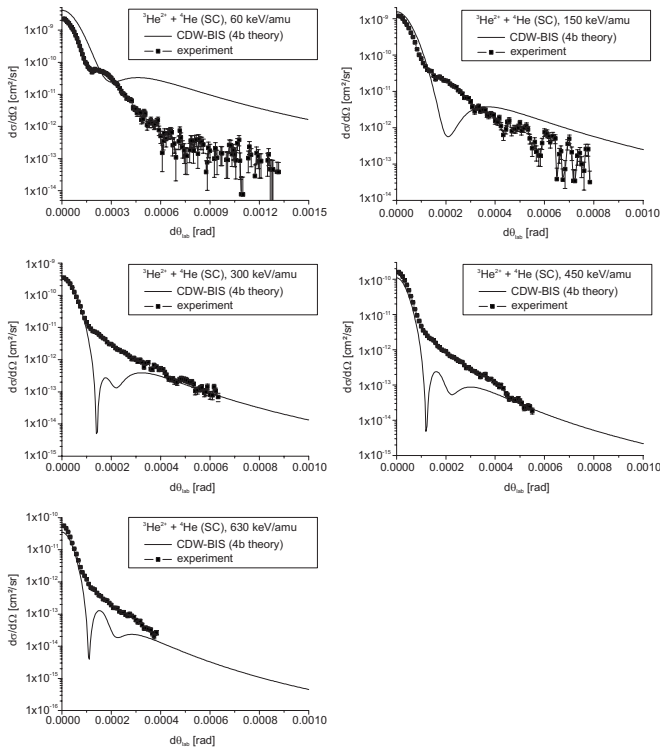


FIG. 3. Differential cross sections $d\sigma_{if}/d\Omega(\text{cm}^2/\text{sr})$ as a function of scattering angle $\theta(\text{rad})$ for single-electron capture to the ground state in He^{2+} -He collisions at 60, 150, 300, 450, and 630 keV/u in the laboratory system. ■: experiment; solid line CDW BIS model (present computation).

strong Thomas peak contribution [$\theta_{lab} = (1/M_P)\sin 60^\circ \approx 0.472$ mrad] with increasing v_P , which is clearly not present in the data and has also not been observed by others in this energy regime. The lowest reported energy with indication of Thomas scattering is above the projectile velocities of 10 a.u. [30].

Theoretical results for single-electron capture in ${}^3\text{He}^{2+} + \text{He}$ collisions at impact energies 60, 150, 300, 450, and 630 keV/u obtained by means of four-body CDW BIS model are compared to the measured data in Fig. 3. The Thomas peak for this collision system would appear at $\theta_{lab} \approx 0.154$ mrad. The CDW BIS model exhibits an unphysical and experimentally unobserved dip before and after the Thomas peak region due to mutual cancellation among the various terms in the perturbation potential. Despite the proper inclusion of the Rutherford scattering, the CDW BIS approximation fails in the region where the nuclear scattering takes over. The experimental resolution is clearly good enough to resolve the predicted structures, if they exist.

The results for differential cross sections in ${}^3\text{He}^+ + \text{He}$ collisions are displayed in Fig. 4. In this five-body problem our model only accounts for the presence of the projectile electron through its screening effect. The neutral two-electron atom in the exit channel is described by a hydrogenic model. The fixed effective charge for the projectile does not produce the correct experimental binding energy and it also cannot reflect the true dynamic situation of the captured electron in the newly formed helium atom. It should be noted that the reduction from a five-body to the four-body problem is crude

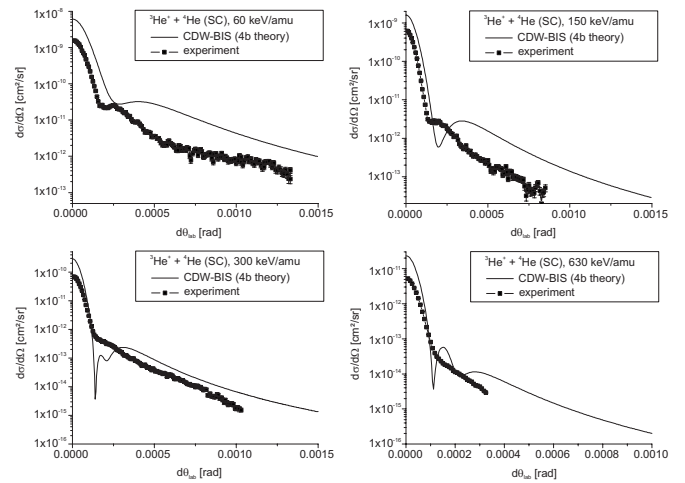


FIG. 4. The differential cross sections $d\sigma_{if}/d\Omega(\text{cm}^2/\text{sr})$ as a function of scattering angle $\theta(\text{rad})$ for single-electron capture to the ground state in He^+ -He collisions at 60, 150, 300, and 630 keV/u in the laboratory system. ■: experiment; solid line CDW BIS model (present computation).

and corresponding results should be used only for rough estimation. The results of the computation, using CDW BIS theory, of such a model reaction are shown in Fig. 4. As expected this theoretical approach yields rather poor agreement with the data. At larger scattering angle we find a similar disagreement as for the collision systems discussed previously. But now, also in the small-angle regime (“the electronic peak”), the v_P dependence is not well predicted. Similar to the impact of He^{2+} the theory shows an unphysical dip around the Thomas peak.

Theoretical results for differential cross sections in ${}^3\text{He}^{2+} + \text{He}$ collisions at incident energies 60, 150, 200, and 300 keV/u are displayed in Fig. 5. The present BDW-calculation computations for double capture are performed by using one-parameter orbitals of the Hylleraas type [23] in

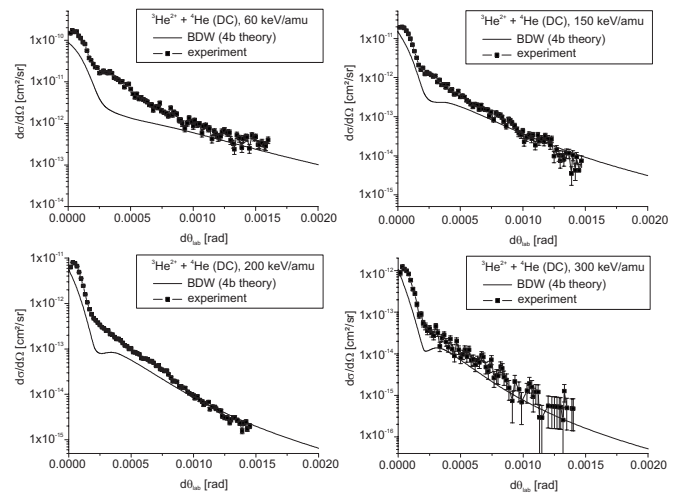


FIG. 5. The differential cross sections $d\sigma_{if}/d\Omega(\text{cm}^2/\text{sr})$ as a function of scattering angle $\theta(\text{rad})$ for double-electron capture to the ground state in He^{2+} -He collisions at 60, 150, 200, and 300 keV/u in the laboratory system. ■: experiment; solid line BDW model (present computation).

both the entrance and exit channels. The behavior of the angular distribution obtained in a four-body boundary-corrected continuum intermediate-state (BCIS) model [31] is altogether quite similar to that in the BDW approximation for the present impact energies. The calculations underestimate in general the experimental data, especially at lower energies. At larger scattering angles (nuclear scattering), experimental and theoretical slopes differ slightly. It should be noted that the displayed theoretical and experimental results are only for the transition $1s^2 \rightarrow 1s^2$.

V. CONCLUSIONS

In conclusion we have presented a systematic comparison of experimental data and theories for fully differential data of the most simple capture reactions in an intermediate range of projectile energies. At very small angles, which are the dominant contribution to the total capture cross section, the trans-

verse momentum exchange in electron transfer is mediated by the electron in the initial state, yielding a universal shape for all systems investigated. Theory and experiment agree best for the impact of protons. Theory always overestimates the influence of the Thomas peak, which is not present in any of the experimental data and has only been seen clearly at very high impact energies 7.5 MeV/u H^+ -He by Fischer *et al.* [5]. At larger scattering angles, where nuclear scattering dominates, theory has trouble matching the experimental details. These findings agree with similar conclusions drawn in the last few years from ionization collisions [32].

We are grateful for help from M. Prior. This work was supported in part by Bundesministerium für Bildung und Forschung (BMBF), Deutsche Forschungsgemeinschaft (DFG), and Roentdek Handels GmbH. I.M. acknowledges the support from Ministry of Science of the Republic of Serbia through Project No. 141029A.

-
- [1] Dž. Belkić, I. Mančev, and J. Hanssen, *Rev. Mod. Phys.* **80**, 249 (2008).
- [2] J. R. Oppenheimer, *Phys. Rev.* **31**, 349 (1928).
- [3] H. C. Brinkman and H. A. Kramers, *Proc. K. Ned. Akad. Wet.* **33**, 973 (1930).
- [4] L. H. Thomas, *Proc. R. Soc. London, Ser. A* **114**, 561 (1927).
- [5] D. Fischer, K. Stochkel, H. Cederquist, H. Zettergren, P. Reinhard, R. Schuch, A. Källberg, A. Simonsson, and H. T. Schmidt, *Phys. Rev. A* **73**, 052713 (2006).
- [6] E. Horsdal-Pedersen, C. L. Cocke, and M. Stöckli, *Phys. Rev. Lett.* **50**, 1910 (1983).
- [7] V. Mergel, R. Dörner, M. Achler, K. Khayyat, S. Lencinas, J. Euler, O. Jagutzki, S. Nüttgens, M. Unverzagt, L. Spielberger, W. Wu, R. Ali, J. Ullrich, H. Cederquist, A. Salin, C. J. Wood, R. E. Olson, Dž. Belkić, C. L. Cocke, and H. Schmidt-Böcking, *Phys. Rev. Lett.* **79**, 387 (1997).
- [8] V. Mergel, R. Dörner, J. Ullrich, O. Jagutzki, S. Lencinas, S. Nüttgens, L. Spielberger, M. Unverzagt, C. L. Cocke, R. E. Olson, M. Schulz, U. Buck, E. Zanger, W. Theisinger, M. Isser, S. Geis, and H. Schmidt-Böcking, *Phys. Rev. Lett.* **74**, 2200 (1995).
- [9] J. Ullrich, R. Moshhammer, R. Dörner, O. Jagutzki, V. Mergel, H. Schmidt-Böcking, and L. Spielberger, *J. Phys. B* **30**, 2917 (1997).
- [10] R. Dörner, V. Mergel, O. Jagutzki, L. Spielberger, J. Ullrich, R. Moshhammer, and H. Schmidt-Böcking, *Phys. Rep.* **330**, 95 (2000).
- [11] J. Ullrich, R. Moshhammer, A. Dorn, R. Dörner, L. Ph. H. Schmidt, and H. Schmidt-Böcking, *Rep. Prog. Phys.* **66**, 1463 (2003).
- [12] O. Jagutzki, J. S. Lapington, L. B. C. Worth, U. Spillman, V. Mergel, and H. Schmidt-Böcking, *Nucl. Instrum. Methods Phys. Res. A* **477**, 244 (2002).
- [13] R. Dörner, V. Mergel, L. Spielberger, M. Achler, Kh. Khayyat, T. Vogt, H. Bräuning, O. Jagutzki, T. Weber, J. Ullrich, R. Moshhammer, M. Unverzagt, W. Schmitt, H. Khemliche, M. H. Prior, C. L. Cocke, J. Feagin, R. E. Olson, and H. Schmidt-Böcking, *Nucl. Instrum. Methods Phys. Res. B* **124**, 225 (1997).
- [14] C. F. Barnett, in *Atomic Data for Fusion, Collisions of H, H₂, He, and Li Atoms with Atoms and Molecules*, edited by I. Alvarez, C. Cisneros, and R. A. Phaneuf (Controlled Fusion Atomic Data Center, Springfield, 1990), Vol. 1.
- [15] Dž. Belkić, *Nucl. Instrum. Methods Phys. Res. B* **86**, 62 (1994).
- [16] Dž. Belkić, I. Mančev, and M. Mudrinic, *Phys. Rev. A* **49**, 3646 (1994).
- [17] Dž. Belkić and I. Mančev, *Phys. Scr.* **45**, 35 (1992); **47**, 18 (1993).
- [18] Dž. Belkić, *J. Phys. B* **26**, 497 (1993); D. Belkic, *Phys. Rev. A* **47**, 189 (1993).
- [19] I. Mančev, *J. Comput. Methods Sci. Eng.* **5**, 73 (2005).
- [20] I. Mančev, V. Mergel, and L. Schmidt, *J. Phys. B* **36**, 2733 (2003).
- [21] Dž. Belkić, R. Gayet, J. Hanssen, I. Mančev, and A. Nuñez, *Phys. Rev. A* **56**, 3675 (1997).
- [22] J. N. Silverman, O. Platas, and F. A. Matsen, *J. Chem. Phys.* **32**, 1402 (1960).
- [23] E. Hylleraas, *Z. Phys.* **54**, 347 (1929).
- [24] P. Löwdin, *Phys. Rev.* **90**, 120 (1953).
- [25] E. Y. Kamber, C. L. Cocke, S. Cheng, and S. L. Varghese, *Phys. Rev. Lett.* **60**, 2026 (1988).
- [26] R. Dörner, J. Ullrich, H. Schmidt-Böcking, and R. E. Olson, *Phys. Rev. Lett.* **63**, 147 (1989).
- [27] S. W. Bross, S. M. Bonham, A. D. Gaus, J. L. Peacher, T. Vajnai, M. Schulz, and H. Schmidt-Böcking, *Phys. Rev. A* **50**, 337 (1994).
- [28] P. J. Martin, K. Arnett, D. M. Blankenship, T. J. Kvale, J. L. Peacher, E. Redd, V. C. Sutcliffe, J. T. Park, C. D. Lin, and J. H. McGuire, *Phys. Rev. A* **23**, 2858 (1981).
- [29] M. Zapukhlyak, T. Kirchner, A. Hasan, B. Tooke, and M. Schulz, *Phys. Rev. A* **77**, 012720 (2008).
- [30] H. Vogt, R. Schuch, E. Justiniano, M. Schulz, and W. Schwab, *Phys. Rev. Lett.* **57**, 2256 (1986).
- [31] D. Belkic, *Phys. Rev. A* **47**, 3824 (1993).
- [32] M. Schulz, R. Moshhammer, D. Fischer, H. Kollmus, D. H. Madison, S. Jones, and J. Ullrich, *Nature (London)* **422**, 48 (2003).